

Selection of Plate Components of Operator's Cabin Walls in Aspect of Thermal Insulation and Transmission Loss

Zygmunt DZIECHCIOWSKI

Cracow University of Technology
Faculty of Mechanical Engineering
Institute of Machine Design
Jana Pawła II 37, 31-864 Kraków, Poland
e-mail: dziechci@mech.pk.edu.pl

(received April 27, 2010; accepted January 25, 2011)

The modern cabin of heavy duty machines have to fulfil a number of requirements which deal with operators' work comfort. More and more often, the vibroacoustic and thermal comforts decide about the cabin quality. This paper presents principles of acoustic and thermal calculations as well as their use in combined assessment.

Keywords: acoustic and thermal comfort, heavy-duty machine cabin, transmission loss, thermal insulation.

1. Introduction

The ergonomic design of heavy-duty machines should take into consideration influence of many harmful factors which affect the operator such as noise, vibration, thermal environment, dustiness, etc. The control of harmful factor field distribution could be made by changing of the operator's cabin walls structure. This paper describes results of the analysis of influence of plate elements structure on thermal and acoustic condition in the cabin.

2. Acoustic and thermal calculations for single-layer and multilayer plates

2.1. Acoustic calculation

There can be found in literature a relation for prediction of the transmission loss TL in the single-layer and in multilayer plates. Among models for determination of TL for single-layer structure, might be distinguished (CALLISTER *et al.*, 1999): mass law, Cremer's equation, mass law-Sharp-Cremer model and Sewell-Sharp-Cremer model. For multilayer structure might be used the expression derived by SHARP (SHARP *et al.*, 1969) and BOGOLEPOV (1986).

An engineering calculation in aspect of acoustic insulation may base on the so-called mass law. Results of calculation, which are obtained by this method not always find confirmation in an experimental research, because the mass law does not take into account material properties of plate elements structure, which the cab wall consists of. The mass law is valid only below the coincidence frequency. Cremer (1942, cited by CALLISTER *et al.*, 1999, p. 146), derived the expression for the transmission loss calculation of panels above coincidence. For the disparity between the mass law and experiment at frequencies near coincidence, Sharp (1978, cited by CALLISTER *et al.*, 1999, pp. 146–148) proposed an empirical method. Sewell's expression (SEWELL, 1970, cited by CALLISTER *et al.*, 1999, p. 148) enables to determine TL at low frequencies.

In the heavy duty machines, a single-layer structure of cab wall is not very often used. The structures like that can be found in older structure of cabs wall. Even in case of cab windows, a single-layer glass plates are used very seldom.

Multilayer structures are commonly used as plate elements. This paper contains calculation formulas which were defined by SHARP (1969) and BOGOLEPOV (1986).

The relations given by BOGOLEPOV (1986) have applications for structures which contain a sound-absorbing material inside. An example of cross-section for this model is presented in Fig. 1. The calculation formula of an acoustic insulation property r of a plate with three-layer structure (see Fig. 1) is given by the Eq. (1).

The sound intensities before and after the plate is presented in Figs. 1 and 2 as J_1 and J_2 .

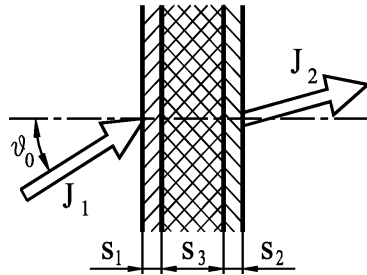


Fig. 1. Cross-section of three-layer structure.

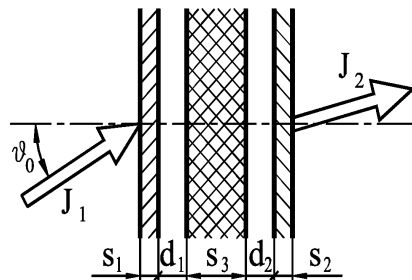


Fig. 2. Cross-section of three-layer structure with separations between double panels.

$$r = \left| \frac{e^{-i \cdot k_0 \cdot s_3 \cdot \cos \vartheta_0}}{4 \cdot Z_0 \cdot Z_3} \cdot (Z_3 + Z_0)^2 \cdot \left\{ \left[\frac{Z_{B1}}{2 \cdot Z_0} \cdot \left(\frac{Z_3 - Z_0}{Z_3 + Z_0} \right) - \left(1 + \frac{Z_{B1}}{2 \cdot Z_0} \right) \right] \right. \right. \\ \times \left[\frac{Z_{B2}}{2 \cdot Z_0} \cdot \left(\frac{Z_3 - Z_0}{Z_3 + Z_0} \right) - \left(1 + \frac{Z_{B2}}{2 \cdot Z_0} \right) \right] \cdot e^{\gamma \cdot s_3 \cdot \cos \vartheta_3} \\ \left. \left. - \left[\frac{Z_{B1}}{2 \cdot Z_0} - \left(1 + \frac{Z_{B1}}{2 \cdot Z_0} \right) \cdot \left(\frac{Z_3 - Z_0}{Z_3 + Z_0} \right) \right] \right. \right. \\ \left. \left. \times \left[\frac{Z_{B2}}{2 \cdot Z_0} - \left(1 + \frac{Z_{B2}}{2 \cdot Z_0} \right) \cdot \left(\frac{Z_3 - Z_0}{Z_3 + Z_0} \right) \right] \cdot e^{-\gamma \cdot s_3 \cdot \cos \vartheta_3} \right\}^2 \right|, \quad (1)$$

where

- s_1, s_2, s_3 – dimensions of plate element according to Fig. 1, [m],
- $\rho_0, \rho_1, \rho_2, \rho_3$ – density of air (subscripts 0), external plate (subscript 1 and 2) and porous material (subscript 3), [kg/m³],
- Z_0 – the acoustic impedance of air, $Z_0 = \rho_0 \cdot c_0$, [kg/(m³·s)],
- Z_3 – the acoustic impedance of porous material, $Z_3 = \rho_3 \cdot c_3 / \cos \vartheta_3$, [kg/(m³·s)],
- c_0 – sound speed in air, [m/s],
- ϑ_0 – the angle of incidence of sound wave on a barrier, [°],
- ω – radian frequency of excitation, [rad/sec],
- μ_1, μ_2 – surface mass-density of outer plates, [kg/m²],
- Z_{B1}, Z_{B2} – the acoustical impedance of outer plates,

$$Z_{B1} = i \cdot \left[\omega \cdot \mu_1 - \frac{E_1 \cdot J_{B1} (1 + i\eta_1) \cdot \omega^3 \cdot \sin^4 \vartheta_0}{c_0^4 \cdot (1 - \nu_1^2)} \right],$$

$$Z_{B2} = i \cdot \left[\omega \cdot \mu_2 - \frac{E_2 \cdot J_{B2} (1 + i\eta_2) \cdot \omega^3 \cdot \sin^4 \vartheta_0}{c_0^4 \cdot (1 - \nu_2^2)} \right],$$

c_3 – complex velocity of wave propagation in porous material, $c_3 = \frac{\alpha_m^2 + \beta_m^2}{\alpha_m + i \cdot \beta_m}$,

γ_m – the propagation coefficient (the constant of wave propagation in porous material), $\gamma_m = \beta_m + i \cdot \alpha_m$, [1/m],

α_m – the attenuation coefficient, [1/m],

β_m – the phase coefficient, [1/m],

ϑ_3 – the angle of refraction of sound wave in the porous material, $\cos \vartheta_3 = \sqrt{1 - (c_3/c_0)^2 \cdot \sin^2 \vartheta_0}$, [-],

J_{B1}, J_{B2} – moment of inertia of external plates, which are of unitary width, $J_{B1,2} = s_{1,2}^3/12$, [m³],

$E_1, E_2, \nu_1, \nu_2, \eta_1, \eta_2$ – Young's modulus, [MPa], Poisson's ratio [-] and loss factor [-] for external plates.

The acoustic insulation property of a barrier r_D in the diffuse field is obtained by:

$$r_D = \frac{\int_0^{\vartheta_{\text{lim}}} \cos \vartheta_0 \cdot \sin \vartheta_0 \, d\vartheta_0}{\int_0^{\vartheta_{\text{lim}}} \frac{\cos \vartheta_0 \cdot \sin \vartheta_0}{r} \, d\vartheta_0}. \quad (2)$$

Transmission loss is determined by:

$$TL = 10 \cdot \log r_D \quad [\text{dB}]. \quad (3)$$

Sharp's equation has no limitation in aspect of material-type inside sandwich panel, that is why it is more universal. The cross-section of a three-layer structure for Sharp's model is shown in Fig. 2. The expression for calculation of the transmission coefficient is given by equation:

$$T = \frac{-T_1 \cdot T_3 \cdot \exp\left(-i \cdot k_y \cdot \frac{d_1 + d_2}{2}\right)}{R_1 \cdot R_3 \cdot \left\{ T_2 - \frac{1}{T_2} \left[\frac{\exp(-2i \cdot k_y \cdot d_2)}{R_3} - R_2 \right] \cdot \left[\frac{\exp(-2i \cdot k_y \cdot d_1)}{R_1} - R_2 \right] \right\}}, \quad (4)$$

where

- d_1, d_2 – distance between double panels (Fig. 2), [m],
- k_y – propagation constant in y -direction, $k_y = \omega \cdot c_0^{-1} \cdot \cos \vartheta_0$, [rad/m],
- k_x – propagation constant in x -direction, $k_x = \omega \cdot c_0^{-1} \cdot \sin \vartheta_0$, [rad/m],
- T_1, T_2, T_3 – plane wave transmission coefficients for each panel,
- R_1, R_2, R_3 – plane wave reflection coefficients for each panel,
- ϑ_{lim} – upper limit for angle of incidence, [°],

$$T_{1,2,3} = -C_{1,2,3} (Z_{B\ 1,2,3} + Z_{E\ 1,2,3}) \cdot \frac{\cos \vartheta_0}{2 \cdot \rho_0 \cdot c_0},$$

$$R_{1,2,3} = -C_{1,2,3} \left(1 + Z_{B\ 1,2,3} \cdot Z_{E\ 1,2,3} \cdot \frac{\cos^2 \vartheta_0}{4 \cdot \rho_0^2 \cdot c_0^2} \right),$$

$$C_{1,2,3} = \frac{1}{\left[1 + Z_{B\ 1,2,3} \cdot \frac{\cos \vartheta_0}{2 \cdot \rho_0 \cdot c_0} \right] \cdot \left[1 + Z_{E\ 1,2,3} \cdot \frac{\cos \vartheta_0}{2 \cdot \rho_0 \cdot c_0} \right]},$$

$$Z_{B\ 1,2,3} = \frac{i \cdot 8 \cdot \rho_{1,2,3} \cdot c_s^4_{1,2,3}}{\omega^3} \cdot \left(\beta_{1,2,3} \cdot k_x^2 \cdot \tanh\left(\frac{\beta_{1,2,3} \cdot s_{1,2,3}}{2}\right) - \left(k_x^2 - \frac{\omega^2}{2c_s^2_{1,2,3}}\right)^2 \cdot \frac{\tanh\left(\frac{\alpha_{1,2,3} \cdot s_{1,2,3}}{2}\right)}{\alpha_{1,2,3}} \right),$$

$$Z_{E\ 1,2,3} = \frac{i \cdot \rho_{1,2,3} \cdot c_s^4_{1,2,3}}{\omega^3} \cdot \left(-\beta_{1,2,3} \cdot k_x^2 \cdot \coth\left(\frac{\beta_{1,2,3} \cdot s_{1,2,3}}{2}\right) - \left(k_x^2 - \frac{\omega^2}{2c_s^2_{1,2,3}}\right)^2 \cdot \frac{\coth\left(\frac{\alpha_{1,2,3} \cdot s_{1,2,3}}{2}\right)}{\alpha_{1,2,3}} \right),$$

$$\alpha_{1,2,3}^2 = k_x^2 - \frac{\omega^2}{c_c^2_{1,2,3}}, \quad \beta_{1,2,3}^2 = k_x^2 - \frac{\omega^2}{c_s^2_{1,2,3}},$$

c_s – velocity of shear waves for plate element material, [m/s],

$$c_{s\ 1,2,3} = \sqrt{\frac{E_{1,2,3}}{2 \cdot \rho_{1,2,3} \cdot (1 + \nu_{1,2,3})}},$$

c_c – velocity of compression waves for plate element material, [m/s],

$$c_{c\ 1,2,3} = \sqrt{\frac{E_{1,2,3} \cdot (1 - \nu_{1,2,3})}{\rho_{1,2,3} \cdot (1 + \nu_{1,2,3}) \cdot (1 - 2\nu_{1,2,3})}},$$

s_1, s_2, s_3 – thickness of plate elements according to Fig. 2, [m],
 E_1, E_2, E_3 – Young's modulus of plate element material, [MPa],
 ν_1, ν_2, ν_3 – Poisson's ratio of plate element material, [-],
 ρ_1, ρ_2, ρ_3 – density of barrier plate element, [kg/m³].

The random incidence average transmission coefficient is given by the formula

$$\langle T^2 \rangle = \frac{\int_0^{\vartheta_{\text{lim}}} |T|^2 \cdot \sin 2\vartheta_0 \, d\vartheta_0}{\int_0^{\vartheta_{\text{lim}}} \sin 2\vartheta_0 \, d\vartheta_0}. \quad (5)$$

Transmission loss is determined by

$$TL = -10 \cdot \log \langle T^2 \rangle \quad [\text{dB}]. \quad (6)$$

In the calculations to be presented here, the Eq. (5) was calculated for the limiting angle ϑ_{lim} from 0° to 80°.

The presented formulas might be useful in acoustic computation of the specific wall structure and may make preliminary selection of a type structure faster.

The equations for calculation of the transmission loss are limited by the range of application. The boundary of these is the so-called coincidence frequency f_c . The equation for calculation of coincidence frequency f_c is given by

$$f_c = \frac{c_0^2}{2\pi} \sqrt{\frac{\mu}{D}} \quad [\text{Hz}], \quad (7)$$

where D – stiffness of plate element, [Nm], μ – surface mass-density of plate element, [kg/m²].

For the plate that consists of a one-layer structure, stiffness can be calculated from the formula

$$D_{1_w} = \frac{E_1 \cdot s_1^3}{12 \cdot (1 - \nu_1^2)} \quad [\text{Nm}], \quad (8)$$

whereas for a two-layers structure could be taken the approximate formula (9) (CREMER, HECKL, 1988).

$$D_{2_w} \approx \frac{E_1 \cdot s_1^3}{12} + E_3 \cdot s_3 \cdot \left(\frac{s_3 + s_1}{2} \right)^2 \quad [\text{Nm}]. \quad (9)$$

The second term of formula (9) is significant only when $s_3 > s_1$.

One or two coincidence frequencies occur for three-layers structure. The bending stiffness of structures like that, in case of $s_1 = s_2$, is defined by expressions (10) and (11) (BREMNER, O'KEEFFE, 1985).

$$D_{3_w-I} = \frac{E_1 \cdot s_1 \cdot (s_1 + s_3)^2}{2 \cdot (1 - \nu_1^2)} \quad [\text{Nm}], \quad (10)$$

$$D_{3_w-II} = \frac{E_1 \cdot s_1^3}{6 \cdot (1 - \nu_1^2)} \quad [\text{Nm}]. \quad (11)$$

In the expressions (8)–(11) E_1 denotes the Young's modulus of outer plates, [MPa], and E_3 – the Young's modulus of a porous material, [MPa].

If the transmission loss for each plate element is known, it is possible to calculate the transmission loss for the all cab structure, according to relation (12) (PUZYNA, 1974),

$$R_{EK} = 10 \cdot \log \frac{\sum_{i=1}^n \alpha_i \cdot S_i}{\sum_{k=1}^m \gamma_k \cdot S_k} \quad [\text{dB}], \quad (12)$$

where $\sum_{i=1}^n \alpha_i \cdot S_i$ – the total acoustic absorption of cabin walls, [m²], $\sum_{k=1}^m \gamma_k \cdot S_k$ – the total sound transmission of cabin walls, [m²].

2.2. Thermal data

The thermal calculation might be limited by evaluation of the heat transmission coefficient k for a single-layer structure and for “sandwich” type of the structure. This coefficient is dependent on the convective heat transmission coefficient α_c (in case of operator’s cab – may be different for both sides of the barrier), the thickness of plate element s and the heat conduction λ_c . Information concerning material properties allow to calculate overall heat transmission coefficient value k_{all} for any structures of cabin wall, which is defined as:

$$k_{all} = \frac{1}{\frac{1}{\alpha_{c1}} + \sum_{i=1}^n \frac{s_i}{\lambda_{ci}} + \frac{1}{\alpha_{c2}}} \quad [\text{W}/\text{m}^2 \cdot \text{K}], \quad (13)$$

where s_i – thickness of each plate element, [m], λ_{ci} – heat conduction of each plate element, [W/m·K], α_{c1} , α_{c2} – the convective heat transmission coefficients for each side of the plate, [W/m²·K].

3. Results of calculation for different structures of cabin wall

The calculation were divided into two parts. The first part was done for comparison of the results of computer simulation and measurements of the investigated structure (SADOWSKI, 1973; ZAJAC, 2000). The second parts were done in order to define a suitable approach for combined assessment.

The computations were conducted for structures which are a combination of an aluminium plate and a porous rubber plate (porous material), as well as for the structure made of glass. Table 1 presents material properties of the simulated structures shown in Figs. 3 and 5. The material properties of investigated structure were taken from the literature (BIES, HANSEN, 2003; ENGEL, 1993; Polish Standard, 1991).

Table 1. The material properties of calculated structure.

	Young’s modulus E [MPa]	Poisson’s ratio ν [-]	Heat conduction λ_c [W/m·K]	Density ρ [kg/m ³]
Aluminium	70000	0.33	200	2700
Porous rubber	1.0	0.40	0.033	560
Glass	67600	0.22	0.8	2500

In the acoustic computation was used the formula (6) (SHARP *et al.*, 1969). There are presented in the Figs. 4 and 6 graphs of transmission loss of the investigated structures (Figs. 3 and 5). Continuous line shows transmission loss TL which was calculated, whereas the dashed line shows the result of a measurement (SADOWSKI, 1973; ZAJAC, 2000).

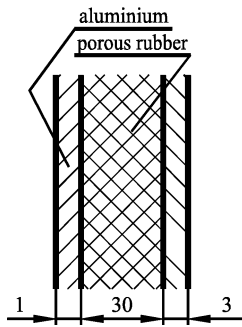


Fig. 3. Cross-section of the structure.

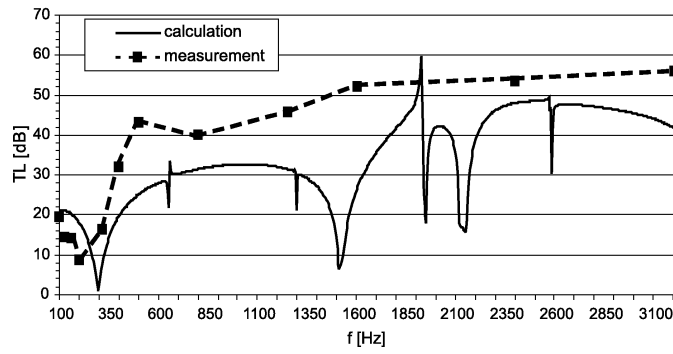


Fig. 4. The transmission loss TL of cabin wall structure (Al – porous rubber – Al).

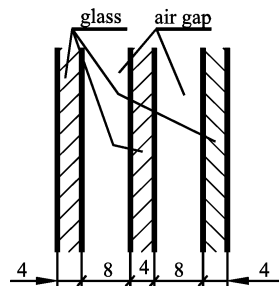


Fig. 5. Cross-section of the calculated structure.

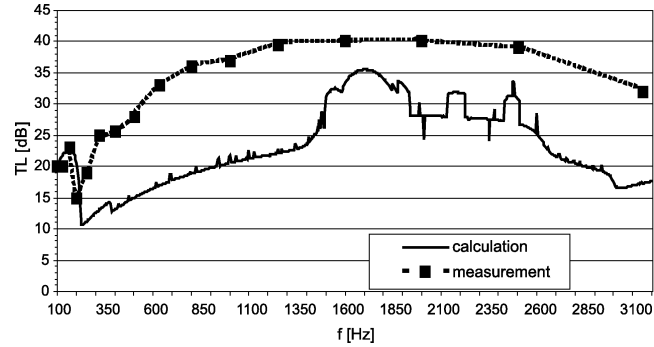


Fig. 6. The transmission loss TL of the calculated cabin wall structure (glazed system 4/8/4/8/4).

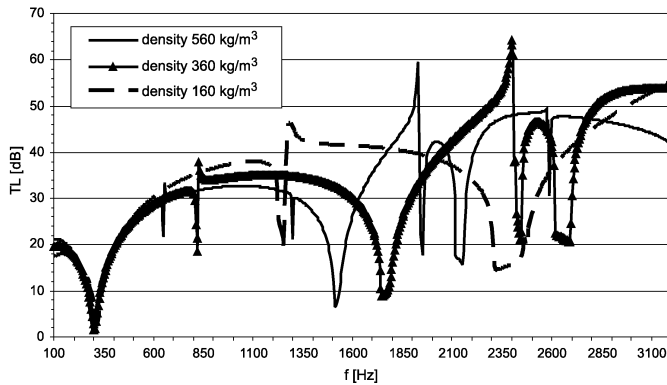


Fig. 7. The transmission loss TL of calculated cabin wall structure (Al – porous rubber – Al) for different densities of porous rubber.

After analysis of the graphs shown in Figs. 4 and 6 it can be noticed, that the results of TL calculations according to (6) and measurements taken from literature, show a similarity of shape. It can be seen that between the results of

measurements and calculations of acoustic insulation appears difference in values. For the structure shown in Fig. 3, measurement TL values are larger than the calculated one. The average differences about 10 dB. For a structure made of glass (Fig. 5), the measured values are larger than those calculated also and the average differences are about 15 dB.

The influence of material properties on TL value were also simulated. The change of transmission loss of structure, as a function of frequency, for different densities of porous material (porous rubber) is presented in Fig. 7. It can be noticed that increase of porous material density causes increase of transmission loss value. Increase of porous material density also causes displacing of the resonance frequencies. The differences between the transmission loss values which were obtained by measurement and computation, can be caused by distinction in measured and calculated material properties.

The second parts of calculations consist of thermal and acoustic simulations for combined assessment of the operator's cab. The simulations were carried out for various thicknesses of porous material (for thickness in the range of 5 to 55 mm) and for constant values of the other parameters of the plates. The calculated structure was the structure, a cross-sectional view of which is shown in Fig. 3.

The thermal calculations were made under assumption that heat flux is perpendicular to the surface of the material. The convective heat-transfer coefficients values, for both sides of plates, are different and are as follows: $\alpha_{c1} = 22.7 [W/m^2 \cdot K]$, $\alpha_{c2} = 7.9 [W/m^2 \cdot K]$ (SZEWCZYK *et al.*, 1991). The convective heat-transfer coefficient values are related to external and internal sides of the plate, adequately.

The acoustic simulations were done for diffused wave action on the material surface.

In the Fig. 8 is presented the graph of change of transmission loss TL and k factor as a function of porous material thickness, in case of the three-layer struc-

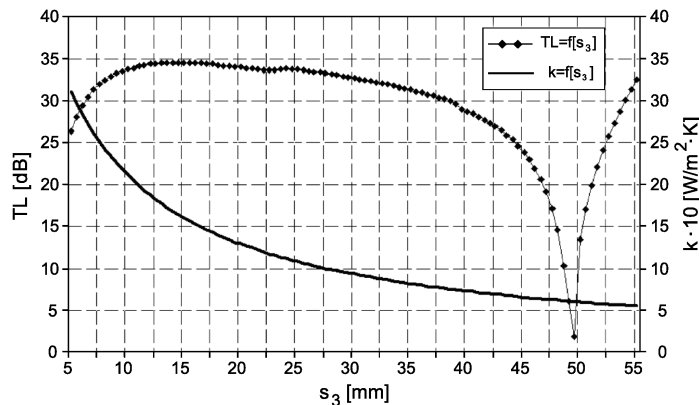


Fig. 8. The heat transmission coefficient k and the transmission loss TL for different thickness s_3 of porous material (for wall made of aluminium plate – porous rubber plate – aluminium plate) – result of calculations.

ture. It can be seen that increase of thickness of the core (in the range of about 10 to 50 mm) is not connected with increase of transmission loss. Above the thickness of 30 mm the TL decrease and enlarge dimension of porous rubber is not cost – effective. In range of thickness of 30 to 55 mm the value of overall heat transmission coefficient decrease imperceptibly.

4. Conclusions

The operator's cab design is a complex process and it is necessary to take into consideration a lot of factors such as: noise, vibrations and thermal factors. Building of a complicated computational model is very time-consuming process. In this paper the computational procedure is proposed, which allows to predict acoustic and thermal insulation of cab walls during preliminary selection of the plate element material. For simulation was chosen the formula, which was presented by SHARP *et al.* (1969).

In comparison with the relation described by BOGOLEPOV (1986), it requires use of a primary material properties, which include catalogue cards. The results of TL calculation and measurements taken from the literature (ZAJAC, 2000; SADOWSKI, 1973) (Figs. 4 and 6) show similarity of shape. With the help of the Sharp's procedure, computation of investigated structure was done due to the influence of porous material density on transmission loss. Effects of calculation confirm results of the other (URIS *et al.*, 1999) and according to them, density not always has advantageous influences on the TL of structure.

Multicriterion design allows to take into account influence of more than one harmful factor. The graph relation between the transmission loss TL and k factor as a function of porous material thickness, which is shown in Fig. 8, allows to select a suitable material easily for specific case.

The formulas which are presented in this paper allow to estimate the possibilities of multi-layer structures application as a plate element of cabin wall, both during design process and in case of verification of the existing structure.

This paper is a part of the project which deals with an engineering application of multi-layer structures as plate elements of the operator's cabin.

References

1. BIES D.A., HANSEN H.H. (2003), *Engeneering Noise Control. Theory and Practice*, 3th Ed., Spon Press, London and New York.
2. BOGOLEPOV I.I. (1986), *Industrial Acoustic Insulation* [in Russian], Sudostroenie, Leningrad.
3. BREMNER, O'KEEFFE (1985), *Calculation of Transmission Loss and Radiation Efficiency of Honeycomb Panels using Finite Element Methods*, SDRC Report #85078 A, Hitchin, UK.

4. CALLISTER J.R., GEORGE A.R., FREEMAN G.E. (1999), *An Empirical Scheme to Predict the Sound Transmission Loss of Single-Thickness Panels*, *Journal of Sound and Vibration*, **222**, 1, 145–151.
5. CREMER L., HECKL M. (1988), *Structure – Borne Sound. Structural Vibrations and Sound Radiation at Audio*, Second Edition, Springer–Verlag Berlin – Heidelberg – New York – London – Paris – Tokyo.
6. ENGEL Z. (1993), *Environmental Noise and Vibration Protection* [in Polish: *Ochrona środowiska przed drganiami i hałasem*], PWN, Warszawa.
7. PN-91/B-02020, *Thermal Protection of Buildings – Requirements and Calculations* [in Polish: *Ochrona cieplna budynków. Wymagania i obliczenia.*].
8. PUZYNA Cz. (1974), *Noise Control in Industry. Selected problems* [in Polish: *Zwalczanie hałasu w przemyśle. Zasady ogólne*], WNT, Warszawa.
9. SADOWSKI J. (1973), *Fundamentals of acoustical insulation of structures* [in Polish: *Podstawy izolacyjności akustycznej ustrojów*], PWN, Warszawa.
10. SHARP B.H.S., BEAUCHAMP J.W., FREEMAN G.E. (1969), *The Transmission Loss of Multilayer Structures*, *Journal of Sound and Vibration*, **9**, 1, 383–392.
11. SZEWCZYK K., STOLARSKI B., NIEZGODA B., SZCZYBURA M., CICHOCKI W. (1991), *Cabins of construction equipment meeting the requirements within the range of thermal comfort, Research project PB – 1445/3/91* [in Polish: *Kabiny maszyn budowlanych spełniające wymogi ergonomii w zakresie komfortu cieplnego, Projekt badawczy PB – 1445/3/91*], Kraków.
12. URIS A., LLOPIS A., LLINARES J. (1999), *Effect of the rockwool bulk density on the airborne sound insulation of lightweight double wall*, *Applied Acoustics*, **58**, 327–331.
13. ZAJAC J. (2000), *The Influence of Glass on Airborne Sound Insulation of Window*, *Archives of Acoustics*, **25**, 3, 387–392.